




Hydrogen dissociation degree in the Grimm-type glow discharge measured by optical emission spectroscopy

Milica M. Vasiljević^{1,a} , Gordana Lj. Majstorović², Ivan R. Videnović¹, and Djordje Spasojević¹

¹ Faculty of Physics, University of Belgrade, P.O. Box 44, 11001 Belgrade, Serbia

² University of Defence, Military Academy, Pavla Jurišića Šturma 33, 11105 Belgrade, Serbia

Received 28 February 2023 / Accepted 15 June 2023 / Published online 7 July 2023

© The Author(s), under exclusive licence to EDP Sciences, SIF and Springer-Verlag GmbH Germany, part of Springer Nature 2023

Abstract. The hydrogen dissociation degree is measured by means of optical emission spectroscopy in the cathode sheath of cylindrical abnormal Grimm-type DC glow discharge operating in the hydrogen–argon mixture at low pressure. The degree of dissociation, ranging from 80% in the close vicinity of the cathode and decreasing to 60% towards the negative glow, is obtained from the intensity ratio of the hydrogen Balmer H_γ line and the diagonal Fulcher- α molecular bands. The cathode sheath thickness is extracted from the electric field strength distribution measured using Stark spectroscopy of the hydrogen Balmer H_α line. An electron temperature of 2.7 eV in the negative glow region is estimated by observing the intensity ratio of the diagonal Fulcher- α bands and the H_α line.

1 Introduction

The cathode sheath (CS) of glow discharges (also called cathode fall or cathode dark space) is a low-intensity region next to the cathode surface, where electrons from the cathode gain sufficient energy for the collisional ionization of atoms. This results in the separation of the opposite charges and additional flux of charged particles, electrons towards the bright negative glow region, and ions and charge-exchange generated neutrals towards the cathode. The cathode sheath is also the region where a major voltage drop takes place to create a macroscopic electric field, accelerate charged species, and further sustain the glow discharge [1–4]. Therefore, the processes occurring in this region are most relevant for the applications in spectroscopic analysis and surface processing (e.g. thin film deposition, plasma etching, and depth profiling), as well as in the development of the plasma-based ion and negative hydrogen ion sources [2, 3, 5, 6]. In latter applications, the degree of dissociation plays an important role. The processes leading to hydrogen dissociation in the discharge can be investigated knowing other relevant discharge parameters, and optical emission spectroscopy (OES) provides a simple, non-intrusive, and reliable way to measure them. In our previous work [7], we used OES to measure electric field strength in the cathode sheath and gas temperature distribution in

hydrogen and hydrogen–argon plane cathode Grimm-type DC glow discharge source (GDS).

In this paper, we present the results of the hydrogen degree of dissociation in the cathode sheath and electronic temperature in the negative glow of a Grimm-type GDS in a hydrogen–argon mixture at low pressure, described in detail in [8] and references therein. Throughout the CS region, we used the intensity ratio of the hydrogen Balmer H_γ line and the Fulcher- α molecular band system, as proposed in [9, 10]. The intensity of the Fulcher- α system is determined using all three branches (P, Q, and R) of $d^3\Pi_u, v' = 0, 1, 2, 3 \rightarrow a^3\Sigma^+_g, v'' = 0, 1, 2, 3$ system. The border between the cathode sheath and negative glow (NG) region is determined using previously employed techniques for the measurement of the electric field strength distribution from the spectral profiles of the H_α line [7]. To complete this study we also estimated the electron temperature in the negative glow, using the intensity ratio of the H_α line and Fulcher- α system.

2 Experimental

Let us begin by mentioning some important details regarding the modified Grimm GDS used in this study, whose detailed description is given earlier [11, 12]. The modification of the standard Grimm lamp [13, 14] with a plane cathode adjacent to the hollow cylindrical anode is made following the design of Ferreira et al. [15], by inserting the cathode into the cylindrical anode. This allows, besides conventional OES from the end of the

^ae-mail: milica.vasiljevic@ff.bg.ac.rs (corresponding author)

discharge, in the direction of the discharge axis (so-called end-on), optical observations parallel to the cathode surface through the longitudinal slots in the anode body (side-on). In this way, different zones of the discharge, namely CS and NG, can be optically observed merely by translating the lamp along the discharge axis, resulting in the information on axial distributions of various plasma parameters.

For the particular conditions of this experiment, the discharge with copper cathode is established in the 95/5 per cent hydrogen/argon mixture at a flow of $300 \text{ cm}^3/\text{min}$. At a pressure of 4.5 mbar, the current-stabilized power supply sustained the discharge at 12 mA and 775 V. For side-on observations of the radiation intensity axial distributions and Stark splitting of hydrogen Balmer lines, the source is translated in 0.125 mm steps for the H_α line recordings and 0.250 mm for the H_γ and Fulcher- α system, see schematics in Fig. 1. For hydrogen Balmer lines recording, a plastic linear polarizer parallel with the discharge axis (i.e. electric field direction) is placed between the source and the detection system to select π -polarized Stark components. The light from the particular position along the discharge axis is focused with unity magnification onto the $20 \mu\text{m}$ entrance slit of the 2 m spectrometer with 0.37 nm/mm reciprocal dispersion in the second diffraction order of a 651 g/mm reflection grating, resulting in a Gaussian instrumental profile of 0.014 nm full width at half maximum. Thermoelectrically cooled CCD at -10°C (Hamamatsu, 2048×506 pixels, $12 \times 12 \mu\text{m}$ pixel size) is used as a light detector, and the data are digitally collected and processed. For intensity measurements, the spectrometer-detector system is calibrated by a standard tungsten lamp.

3 Results and discussion

3.1 Distribution of the electrical field strength in the cathode sheath

To conduct our study on the hydrogen dissociation degree distribution in the CS region from the total intensities of the Fulcher- α system and hydrogen Balmer H_γ line, we needed to determine the thickness and boundary of the CS region first. To this end, we used the criteria of the external electric field decrease from the maximum near the cathode surface towards zero at the border with the NG region. Stark polarization spectroscopy of hydrogen Balmer H_α line is used to measure the electric field strength distribution in the CS.

To obtain the electric field value at a given point in the CS, we recorded the H_α π -polarized line profile, see Fig. 2a, and fitted it with the model function (1) from [7]. The model takes into account the entire $H_\alpha(\pi)$ symmetrical Stark splitting manifold, as well as the small central peak which originates from the part of the discharge protruded through the side-on observation anode slot into the field-free region. The fitting procedure takes into account the entire profile of the Stark-split line and yields precise information on the local electric field strength, see also [16]. It should be noted here that the H_γ profile, used in this work for the measurement of the hydrogen dissociation degree, is also Stark-split in the CS, see example in Fig. 2b, and the information on the local electric field could be extracted from the H_γ π -polarized line profile by using a simple spectroscopic formula [11]:

$$E[\text{V/cm}] = 2.51 \times 10^4 \times \Delta\lambda_{p-p} [\text{nm}], \quad (1)$$

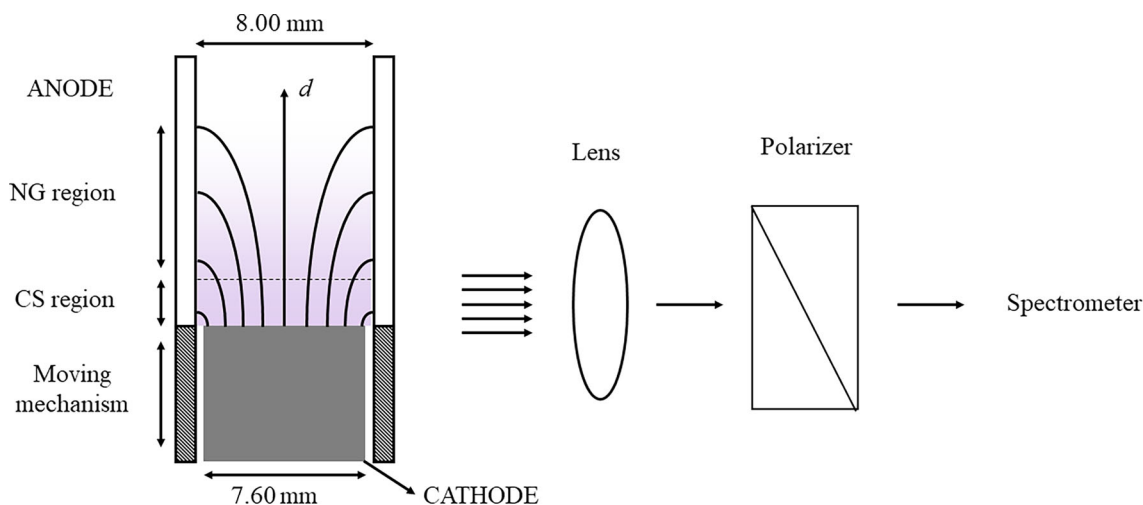


Fig. 1 The central part of modified Grimm GDS and optical set-up for side-on OES

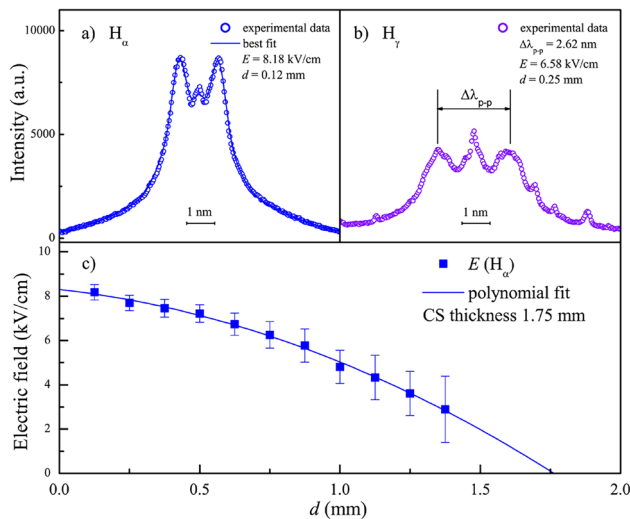


Fig. 2 The examples of side-on recorded π -polarized experimental profiles of the **a** H_{α} line with its best fit (solid line) by the model function [7]; **b** H_{γ} line with indicated peak separation $\Delta\lambda_{p-p}$, Eq. (1). The corresponding values of electric field strength E and distance d from the cathode are given in the legends. **c** Electric field strength axial distribution in the CS region obtained from the H_{α} line together with experimental uncertainties. For better visibility, the uncertainties are enlarged five times. Experimental conditions are given in Sect. 2

where $\Delta\lambda_{p-p}$ is the peak separation, measured from the experimental profile as a distance between convolved Stark components, shifted equally to the red and blue wavelength side, see Fig. 2b. However, due to the low intensity and weaker resolution of Stark components, the electric field values obtained from the H_{γ} line are systematically lower, leading to a discrepancy of about 15% in comparison with the H_{α} results. By polynomial fitting of the electric field distribution obtained from the axial recording of the $H_{\alpha}(\pi)$ profile, we estimated the CS thickness of 1.75 mm, see Fig. 2c.

Although according to the simplest predictions the electric field distribution in the CS region of a glow discharge should be a linear function of the distance to the cathode, numerous experimental findings showed that this need not be the case (see, e.g. [16–19]). The departure from the linearity proved to be a consequence of a series of intertwined causes which have to be analysed in a kinetic approach like, e.g. the iterative kinetic model [18, 19].

As stated in Sect. 3.1, the values of the electric field strength E are obtained as one of the fitting parameters to the experimental profiles of the mentioned model function suitable for the H_{α} spectral line profile. The uncertainty for this (and all other) model function fitting parameter(s) we determined following [20] via Monte Carlo simulations of the synthetic data sets using the experimental uncertainties of the recorded profiles. Within this approach, we took that the uncertainty of each experimental point from a recorded profile is

$\varepsilon_{\text{tot}} = \sqrt{\varepsilon_{\text{sys}}^2 + \varepsilon_{\text{rnd}}^2}$, where ε_{sys} is the systematic error introduced by the detector, while ε_{rnd} is the statistical error calculated at the 95% confidence level from the standard deviation of a series of ten profile measurements at the observed wavelength.

3.2 Fulcher- α diagonal band spectra

Figure 3a illustrates the potential energy curves of the excited states in the H_2 molecule (electronic and vibrational levels) belonging to the Fulcher- α excitation and emission processes, according to data given in [21, 22]. The electron impact on H_2 causes $d^3\Pi_u, v' = 0-3 \leftarrow X^1\Sigma_g^+, v = 0$ transitions, while the radiative transitions $d^3\Pi_u (v', N') \rightarrow a^3\Sigma_g^+ (v'', N'')$ constitute Fulcher- α emissions. For the $H_2 d^3\Pi_u$ state, Λ -doubling causes the rotational levels to split into two components, denoted as $d^3\Pi_u^-$ and $d^3\Pi_u^+$, as shown in Fig. 3b. The spontaneous emission $d^3\Pi_u^- \rightarrow a^3\Sigma_g^+$ results in Q-branch, while $d^3\Pi_u^+ \rightarrow a^3\Sigma_g^+$ constitutes P and R branches, see Fig. 3b. Given the perturbation of the $d^3\Pi_u^+$ state in interaction with $e^3\Sigma_u^+$, the transition probabilities for P and R branches differ from Hönl-London factors [23–25], and the Q-branch of the Fulcher- α hydrogen band is therefore considered more suitable for, e.g. temperature distribution measurements in the CS region [7]. Vibrational term values in certain electronic states are given in [26].

Figure 4 shows experimental spectra of P, Q, and R branch lines of the Fulcher- α diagonal bands with a) $\nu' = \nu'' = 0$ and b) $\nu' = \nu'' = 1$, respectively, measured in the cathode sheath of our discharge. Clear spectra with distinguished rotational lines (wavelengths from [22]) of P, Q, and R branches in the visible 590–645 nm wavelength region, are obtained. The intensities of all branch lines of the $d^3\Pi_u, \nu' \rightarrow a^3\Sigma_g^+, \nu''$ ($\nu' = \nu'' = 0, 1, 2, 3$) electronic transition are used in this study, see also [7].

3.3 Degree of dissociation

Not many studies can be found about the hydrogen dissociation degree in the literature. Most of the studies are carried out in pure hydrogen discharges or argon–hydrogen mixtures at significantly different discharge conditions. For example, for the microwave discharge source, the degree of dissociation of hydrogen is found in the range of 30–90% [27], while this value is near 100% for the cascaded arc plasma [28]. For the typical glow discharge/optical emission spectroscopy (GD-OES) conditions in the argon–hydrogen mixture, the estimated value for the degree of dissociation is 67% [29]. It was also reported that the hydrogen dissociation rate in an argon–hydrogen glow discharge is considerably lower than in a pure hydrogen discharge for pressures above 5 Torr [30], which is the pressure range above our experimental conditions.

The degree of dissociation is the ratio of the dissociated fraction and the total amount of the substance.

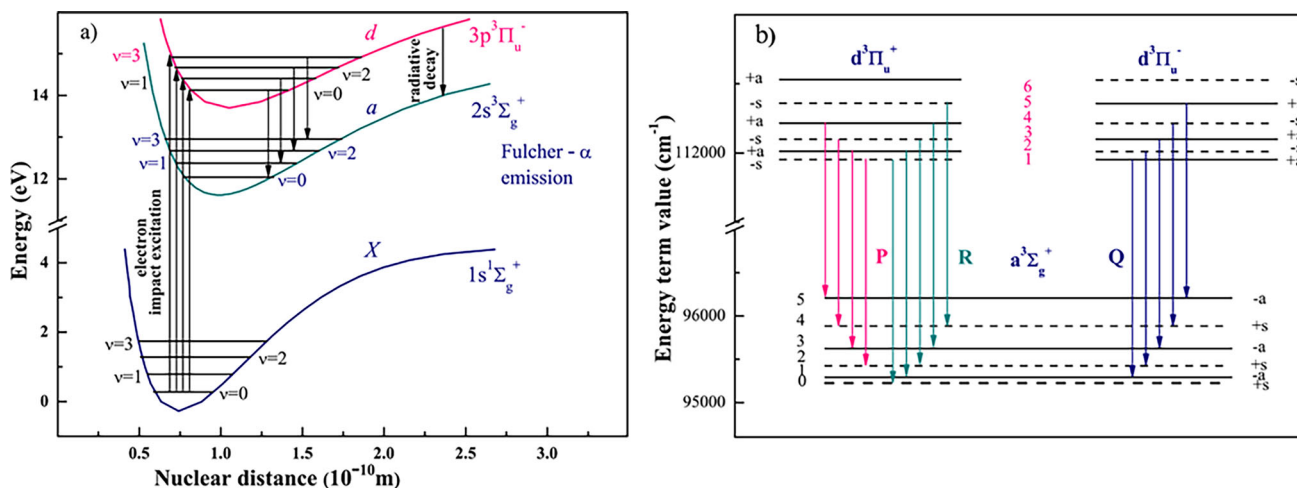


Fig. 3 a Potential curves of the hydrogen molecule with its vibrational states belonging to the Fulcher- α system transitions; b Rotational structure of the Fulcher- α bands system of H_2 for $\nu' = \nu'' = 0$. The data are taken from [21, 22]

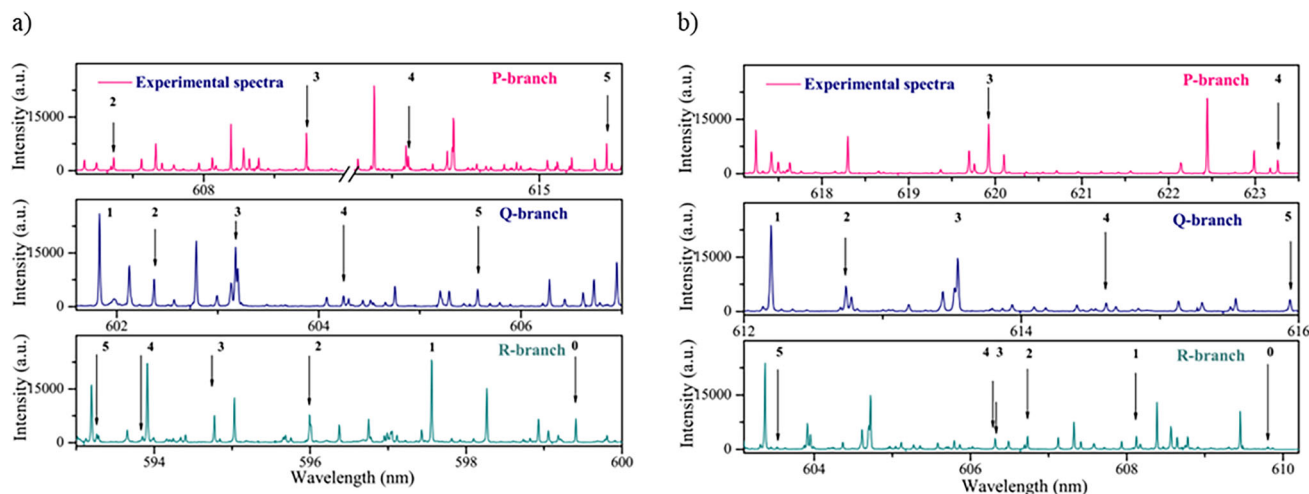


Fig. 4 Several rotational lines in the emission spectra of P, Q, and R-branches of the a $d^3\Pi_u, v' = 0 \rightarrow a^3\Sigma_g^+, v'' = 0$ and b $d^3\Pi_u, v' = 1 \rightarrow a^3\Sigma_g^+, v'' = 1$ band. Experimental conditions are given in Sect. 2

For the hydrogen discharges, it is the ratio between the dissociated hydrogen and the total sum of atomic and molecular hydrogen. The density of the atomic hydrogen is associated with Balmer lines emission, while the molecular radiation corresponds to the emission of molecular radiation (Fulcher- α band transition: $d^3\Pi_u \rightarrow a^3\Sigma_g^+$, $v' = v'' = 0-3$, $\lambda = 590-645$ nm). Some earlier studies [9, 10] indicate that the hydrogen dissociation degree can be estimated from the total intensity ratio of the hydrogen Balmer H_γ line and Fulcher- α system.

The spontaneous emission intensity is the number of photons emitted by a unit volume per second over all directions. The intensity of a spectral line of transition is proportional, in an optically thin case, to the product of the population density of the upper state and the transition probability for spontaneous emission. According to collisional radiative models, the population density depends on the plasma parameters T_e and

n_e , and is proportional to the population coefficients which describe the coupling of the population density to the ground state of the particle. The effective emission rate X^{eff} is the product of population coefficients of the particle and the transition probability for spontaneous emission. Finally, the intensities of atomic and molecular spectral lines are proportional to the densities of atoms [H] or molecules $[H_2]$ multiplied by the corresponding effective emission rates X^{eff} . Thus, for our experimental conditions, we considered the intensity ratio of $H\gamma/H_2$ suitable for the determination of the density ratio between hydrogen atoms and molecules $[H]/[H_2]$.

The intensity ratio, according to [9, 10], is:

$$\frac{I_\gamma}{I_{\text{Ful}}} = \frac{X_\gamma^{\text{eff}} [H]}{X_{H_2}^{\text{eff}} [H_2]}, \tag{2}$$

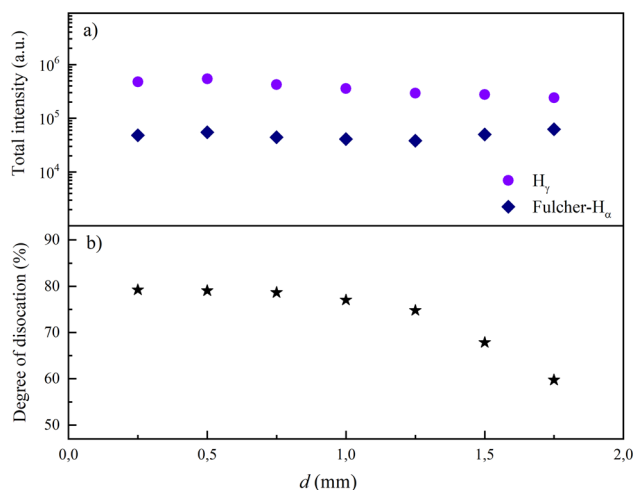


Fig. 5 **a** Total intensities of the H_γ line and Fulcher- α bands ($v' = v'' = 0, 1, 2, 3$) and **b** Dissociation degree of hydrogen against the distance from the cathode through the CS region. Experimental conditions are given in Sect. 2

where X_γ^{eff} and $X_{H_2}^{\text{eff}}$ denote the effective emission rates of the H_γ line and Fulcher- α system, respectively, calculated following the collisional radiative model [9], while $[H]$ and $[H_2]$ stand for the number densities of hydrogen atoms and molecules, respectively. With the high spectral resolution of our optical detection system, we were able to measure the total intensity of the Fulcher- α band and calculate the ratio $\frac{I_\gamma}{I_{H_2}}$. Moreover, according to [9] and references therein, the ratio of the emission rate coefficients $\frac{X_\gamma^{\text{eff}}}{X_{H_2}^{\text{eff}}}$ is barely dependent on the electron temperature T_e and electron density n_e in the range $5 \cdot 10^{16} \text{ m}^{-3}$ – $5 \cdot 10^{18} \text{ m}^{-3}$ and approximately equals 1.3, according to Fig. 5 from [9]. Using this value for the $\frac{X_\gamma^{\text{eff}}}{X_{H_2}^{\text{eff}}}$, the ratio $\frac{[H]}{[H_2]}$ is obtained. Knowing the relationship between the neutral particle density ratio and the degree of dissociation [10, 31], we estimated the degree of dissociation in the cathode sheath as follows:

$$D = \frac{[H]}{[H] + 2[H_2]} = \frac{\frac{[H]}{[H_2]}}{\frac{[H]}{[H_2]} + 2}. \tag{3}$$

Figure 5 presents our results for total intensities of the hydrogen Balmer H_γ line and Fulcher- α system (P, Q, and R branches) throughout the CS region. The results show that the degree of dissociation varies from 60 to 80% and decreases towards the end of the CS region.

3.4 Electron temperature

To understand the behaviour and to model gas discharges and low-density plasmas, it is required to know the values of discharge parameters like, e.g. electron number density, electron temperature and the electron

energy distribution. In Grimm-type glow discharge, earlier measurements performed by a Langmuir probe in argon and neon found excitation temperatures in the range from 0.6 to 0.85 eV for Ar I and 0.5 to 0.9 eV for Ne I [32]. Furthermore, measured excitation temperatures of Ar II were in the range of 3.5–4.4 eV [32], indicating the existence of at least two distinguishable electron groups. Generally three groups of electrons are assumed to exist in a Grimm GDS: the primary group consisting of highly energetic electrons, the group of secondary electrons possibly split into many subgroups, and the group of thermalized electrons. The thermalized and one secondary electron group encountered in the Langmuir probe measurements are reported to have an average energy of 0.5 eV and 4.5 eV, respectively [32]. Another study of the Grimm-type glow discharge using Langmuir probe [33] reports the typical electron temperature of 0.45 eV.

In the negative glow plasma of our Grimm GDS we estimated the electron temperature using the intensity ratio of the Fulcher- α system and hydrogen Balmer line H_α . This spectroscopic method is proposed in [34], assuming that the electron energy distribution function is close to Maxwell's. The main mechanisms of excitation of the $d^3\Pi_u$ state are the electron impact excitation of the hydrogen molecule from the ground state ($d^3\Pi_u \leftarrow X^1\Sigma_g^+$) and the radiative decay into the $a^3\Sigma_g^+$. These two processes are dominant in comparison to cascade processes from higher excited states, collisional deexcitation, and other secondary processes for Fulcher- α system in low-temperature plasmas, see, e.g. [34, 35]. The H_α emission is mainly due to dissociative excitation and dissociative ionization from H_2 molecules by electron impact. For this process, the threshold energy is 13.47 eV while the maximum of its cross section σ_{em} is $(4.2 \pm 0.8) \cdot 10^{-22} \text{ m}^2$ at the electron energy of 15.6 eV, which is close to the threshold of excitation; semiempirically $(7 \pm 2) \cdot 10^{-22} \text{ m}^2$ [35]. The cross sections for the excitation of atomic and molecular lines have different dependencies on electron energy [35, 36], see Fig. 6a. The emission cross section σ_{H_2} has a sharp peak near the threshold energy and decreases rapidly as the excitation energy increases while the σ_{H_α} increases gradually.

The intensity of the Fulcher- α can be expressed as $I_{H_2} = \text{const.} \cdot n_e n_{H_2} \langle \sigma_{H_2} v \rangle$ while for H_α stands: $I_{H_\alpha} = \text{const.} \cdot n_e n_{H_2} \langle \sigma_{H_\alpha} v \rangle$, with the rate coefficients $\langle \sigma_{H_\alpha} v \rangle$ derived from the emission cross sections σ_H using the Maxwellian distribution function:

$$\langle \sigma_H v \rangle = 1.2 \cdot 10^8 \pi^{-\frac{1}{2}} \int_{\Delta E}^{\infty} E \sigma_H T_e^{-\frac{3}{2}} e^{-\frac{E}{T_e}} dE \tag{4}$$

where E and ΔE are the excitation and threshold energy, respectively, and T_e is the electron temperature. The ratio of intensities can be expressed as a relationship of the rate coefficients $I_{H_2}/I_{H_\alpha} = \langle \sigma_{H_2} v \rangle / \langle \sigma_{H_\alpha} v \rangle$ and consequently as a function of the electron temperature. Therefore, the intensity ratio of

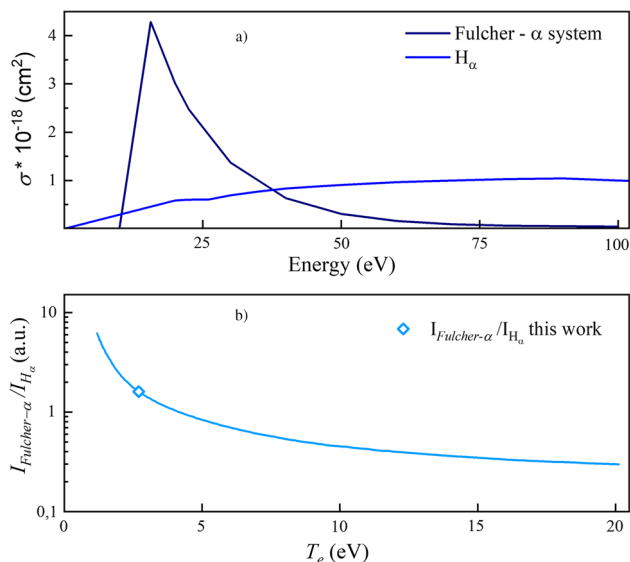


Fig. 6 **a** Excitation functions of the Fulcher- α system and Balmer H_{α} line in the energy range 0–100 eV. The data are taken from [35, 36]. **b** The intensity ratio of the Fulcher- α system to the H_{α} line as a function of electron temperature. The data are taken from [34]

the Fulcher- α system ($d^3\Pi_u-a^3\Sigma_g$) to the H_{α} emission is sensitive to the electron temperature, see Fig. 6b.

The estimated value of the electron temperature T_e in the negative glow in our discharge conditions is 2.7 eV, while the estimated gas temperature is around 900 K, see details in [7]. The addition of hydrogen to an argon discharge has a significant effect on its analytical characteristics inducing, e.g. a change in the electron energy distribution function [29]. This is a possible explanation for T_e being so much higher in an Ar- H_2 discharge than in pure Ar. From the above results, one can consider that the measurement of the intensity ratio of Fulcher- α system to H_{α} emission may be useful for the estimation of the electron temperature in hydrogen discharge at low pressures. Finally, it should be underlined that the theory applied is based on the assumption of direct excitation of spectral transitions by electron impact and dissociative excitation of hydrogen molecules. These processes mostly dominate in a weakly ionized hydrogen plasma at low pressures.

4 Summary and conclusion

This study aims to estimate the degree of dissociation in the CS region and electron temperature in a Grimm-type glow discharge. The intensity of all three branches (P, Q, and R) of the Fulcher- α system, $d^3\Pi_u$, $\nu' = 0, 1, 2, 3 \rightarrow a^3\Sigma_g^+$, $\nu'' = 0, 1, 2, 3$ is used in combination with intensities of $H\gamma$ and H_{α} hydrogen Balmer lines to obtain results. All lines of P, Q, and R

branches of the Fulcher- α system are located in the visible 590–645 nm wavelength region, with sufficient resolution and a high signal-to-noise ratio. The boundary of the cathode sheath is found using Stark spectroscopy for the determination of the electric field strength distribution from the H_{α} line.

To determine the degree of dissociation in the cathode sheath region we used the intensity ratio of the hydrogen Balmer H_{γ} line and Fulcher- α system as suggested in earlier studies [9, 10]. Obtained value varies between 80 and 60% within the cathode sheath region and is comparable with previous results [27–30].

Electron temperature in the negative glow region is estimated from the intensity ratio of the Fulcher- α system and hydrogen Balmer H_{α} line [34]. The estimated electron temperature T_e in the negative glow in our discharge conditions is 2.7 eV, while the estimated gas temperature [7] is around 900 K.

Acknowledgements This work is supported by the Ministry of Science, Technological Development and Innovations of the Republic of Serbia (Grant No. 451-03-47/2023-01/200162). Part of the results was presented at the 31st Summer School and International Symposium on the Physics of Ionized Gases (SPIG), September 5–9, 2022, Belgrade, Serbia. Conference proceedings: <https://publications.aob.rs/102/pdf/spig2022-23-8.pdf>.

Author contribution

MMV contributed to conceptualization, methodology, investigation, and writing. GLM contributed to conceptualization, methodology, investigation, and writing. IRV contributed to conceptualization, methodology, and writing—review. DS contributed to conceptualization, methodology, and supervision.

Data Availability Statement This manuscript has no associated data or the data will not be deposited. [Authors' comment: The datasets supporting the conclusions of this article are available from the corresponding author upon reasonable request.]

Declarations

Conflict of interest The authors declare that they have no known competing financial interests or personal relationships that could have appeared to influence the work reported in this paper.

References

1. A. von Engel, *Ionized Gases* (Oxford Clarendon Press, Oxford, 1965)
2. B. Chapman, *Glow Discharge Processes: Sputtering and Plasma Etching* (Wiley, New York, 1980)

3. R.K. Marcus, J.A. Broeckaert, *Glow Discharge Plasmas in Analytical Spectroscopy* (Wiley, Chichester, 2003)
4. P.F. Little, A. von Engel, The hollow-cathode effect and the theory of glow discharges. *Proc. R. Soc. Lond. A* **224**, 209–227 (1954). <https://doi.org/10.1098/rspa.1954.0152>
5. R.S. Pessoa, L.L. Tezani, H.S. Maciel, G. Petraconi, M. Massi, Study of SF₆ and SF₆/O₂ plasmas in a hollow cathode reactive ion etching reactor using Langmuir probe and optical emission spectroscopy techniques. *Plasma Sources Sci. Technol.* **19**, 025013–025016 (2010). <https://doi.org/10.1088/0963-0252/19/2/025013>
6. M. Bacal, M. Wada, Negative hydrogen ion production mechanisms. *Appl. Phys. Rev.* **2**, 021305 (2015). <https://doi.org/10.1063/1.4921298>
7. M.M. Vasiljević, G.L. Majstorović, Dj. Spasojević, N. Konjević, Q-branch of Fulcher- α diagonal bands for determination of the axial temperature distribution in the cathode sheath region of hydrogen and hydrogen-argon abnormal glow discharge. *J. Quant. Spectrosc. Ra.* **254**, 107195 (2020). <https://doi.org/10.1016/j.jqsrt.2020.107195>
8. D. Spasojević, N.V. Ivanović, N.V. Nedić, M. Vasiljević, N.M. Šišović, N. Konjević, Iterative kinetic model application in diagnostics of argon abnormal DC glow discharges. *Eur. Phys. J. D* **77**, 75 (2023). <https://doi.org/10.1140/epjd/s10053-023-00650-4>
9. U. Fantz, H. Falter, P. Franzen, D. Wunderlich, M. Berger, A. Lorenz, W. Kraus, P. McNeely, R. Riedl, E. Speth, Spectroscopy—a powerful diagnostic tool in source development. *Nucl. Fusion* **46**, S297 (2006). <https://doi.org/10.1088/0029-5515/46/6/S10>
10. J.J. Dang, K.-J. Chung, Y.S. Hwang, A simple spectroscopic method to determine the degree of dissociation in hydrogen plasmas with wide-range spectrometer. *Rev. Sci. Instrum.* **87**, 053503 (2016). <https://doi.org/10.1063/1.4948919>
11. I.R. Videnović, N. Konjević, M.M. Kuraica, Spectroscopic investigations of a cathode fall region of the Grimm-type glow discharge. *Spectrochim. Acta B* **51**, 1707–1731 (1996). [https://doi.org/10.1016/S0584-8547\(96\)01533-9](https://doi.org/10.1016/S0584-8547(96)01533-9)
12. G.L. Majstorović, N.V. Ivanović, N.M. Šišović, S. Djurović, N. Konjević, Ar I and Ne I spectral line shapes for an abnormal glow discharge diagnostics. *Plasma Sources Sci. Technol.* **22**, 045015 (2013). <https://doi.org/10.1088/0963-0252/22/4/045015>
13. W. Grimm, Glimmentladungslampe für spektralanalytische Routinemessungen. *Naturwissenschaften* **54**, 586 (1967). <https://doi.org/10.1007/BF00636820>
14. W. Grimm, Eine neue Glimmentladungslampe für die optische Emissionsspektralanalyse. *Spectrochim. Acta B* **23**, 443–454 (1968). [https://doi.org/10.1016/0584-8547\(68\)80023-0](https://doi.org/10.1016/0584-8547(68)80023-0)
15. N.P. Ferreira, H.G.C. Human, L.R.P. Butler, Kinetic temperatures and electron densities in the plasma of a side view Grimm-type glow discharge. *Spectrochim. Acta B* **35**, 285–295 (1980). [https://doi.org/10.1016/0584-8547\(80\)80092-9](https://doi.org/10.1016/0584-8547(80)80092-9)
16. N.V. Ivanović, N.M. Šišović, Dj. Spasojević, N. Konjević, Measurement of the DC Stark shift for visible Ne I lines and electric field distribution in the cathode sheath of an abnormal glow discharge. *J. Phys. D Appl. Phys.* **50**, 125201–125216 (2017). <https://doi.org/10.1088/1361-6463/aa5c1f>
17. D. Spasojević, S. Mijin, N.M. Šišović, N. Konjević, Spectroscopic application of an iterative kinetic cathode sheath model to high voltage hollow cathode glow discharge in hydrogen. *J. Appl. Phys.* **119**, 053301 (2016). <https://doi.org/10.1063/1.4941267>
18. D. Spasojević, V. Stefleková, N.M. Šišović, N. Konjević, Spectroscopic application of an iterative kinetic model of the cathode-fall region in a hydrogen abnormal glow discharge. *Plasma Sources Sci. Technol.* **23**, 012004 (2014). <https://doi.org/10.1088/0963-0252/23/1/012004>
19. D. Spasojević, N.V. Ivanović, N.V. Nedić, N.M. Šišović, N. Konjević, Complex UV Ne II line shapes in the cathode sheath of an abnormal glow discharge. *Plasma Sources Sci. Technol.* **29**, 085008 (2020). <https://doi.org/10.1088/1361-6595/aba48a>
20. W.H. Press, S.A. Teukolsky, W.T. Vetterling, B.P. Flannery, *Numerical Recipes: The Art of Scientific Computing*, 3rd edn. (Cambridge University Press, Cambridge, 2007)
21. T.E. Sharp, Potential-energy curves for molecular hydrogen and its ions. *Atom. Data Nucl. Data* **2**, 119–169 (1970). [https://doi.org/10.1016/S0092-640X\(70\)80007-9](https://doi.org/10.1016/S0092-640X(70)80007-9)
22. H.M. Crosswhite, *The Hydrogen Molecule Wavelength Tables of Gerhard Heinrich Dieke* (Wiley-Interscience, New York, 1972)
23. G. Herzberg, *Molecular Spectra and Molecular Structure, Spectra of Diatomic Molecules*, vol. 1 (Krieger Publishing Co, Malabar FL, 1989)
24. I. Kovacs, *Rotational Structure in the Spectra of Diatomic Molecules* (Adam Hilger LTD, London, 1969)
25. S.A. Astashkevich, M. Käning, E. Käning, N.V. Kokina, B.P. Lavrov, A. Ohl, J. Röppcke, Radiative characteristics of $3p \Sigma, \Pi; 3d \Pi, \Delta^-$ states of H₂ and determination of gas temperature of low pressure hydrogen containing plasmas. *J. Quant. Spectrosc. Ra.* **56**, 725–751 (1996). [https://doi.org/10.1016/S0022-4073\(96\)00103-3](https://doi.org/10.1016/S0022-4073(96)00103-3)
26. U. Fantz, D. Wunderlich, Franck-condons factors, transition probabilities and radiative lifetimes for hydrogen molecules and their isotopomers, INDC(NDS)-457 (2004)
27. J. Geddes, R.W. McCullough, A. Donnelly, H.B. Gilbody, Dissociation of hydrogen in high-frequency discharges. *Plasma Sources Sci. Technol.* **2**, 93 (1993). <https://doi.org/10.1088/0963-0252/2/2/004>
28. R.F.G. Meulenbroeks, A.J. van Beek, A.J.G. van Helvoort, M.C.M. van de Sanden, D.C. Schram, Argon-hydrogen plasma jet investigated by active and passive spectroscopic means. *Phys. Rev. E* **49**, 4397 (1994). <https://doi.org/10.1103/PhysRevE.49.4397>
29. A. Bogaerts, R. Gijbels, Effects of adding hydrogen to an argon glow discharge: overview of relevant processes and some qualitative explanations. *J. Anal. At. Spectrom.* **15**, 441–449 (2000). <https://doi.org/10.1039/A909779A>
30. M. Capitelli, M. Dilonardo, Nonequilibrium vibrational populations of diatomic species in electrical discharges: effects of the dissociation rates. *Chem. Phys.* **24**, 417–427 (1977). [https://doi.org/10.1016/0301-0104\(77\)85102-1](https://doi.org/10.1016/0301-0104(77)85102-1)

31. B.P. Lavrov, N. Lang, A.V. Pipa, J. Röpcke, On determination of the degree of dissociation of hydrogen in non-equilibrium plasmas by means of emission spectroscopy: II. Experimental verification. *Plasma Sources Sci. Technol.* **15**, 147 (2006). <https://doi.org/10.1088/0963-0252/15/1/021>
32. A. Bogaerts, A. Quentmeier, N. Jakubowski, R. Gijbels, Plasma diagnostics of an analytical Grimm-type glow discharge in argon and in neon: langmuir probe and optical emission spectrometry measurements. *Spectrochim. Acta B* **50**, 1337 (1995)
33. Z. Weiss, Emission spectroscopic diagnostics of weakly ionized argon-diluted plasmas: glow discharge and inductively coupled plasma. *Plasma Sources Sci. Technol.* **29**, 105018 (2020). <https://doi.org/10.1088/1361-6595/abb41e>
34. K. Kondo, K. Okazaki, H. Oyama, T. Oda, Y. Sakamoto, A. Iiyoshi, Electron temperature measurement using Fulcher- α ($d^3\Pi_u-a^3\Sigma_g$) to H_α emissions in a weakly ionized plasma. *Jap. J. Appl. Phys.* **27**, 1560 (1988). <https://doi.org/10.1143/JJAP.27.1560>
35. G.R. Möhlmann, F.J. de Heer, Emission cross sections of the $H_2(3p^3\Pi_u \rightarrow 2s^3\Sigma_g^+)$ transition for electron impact on H_2 . *Chem. Phys. Lett.* **43**, 240–244 (1976). [https://doi.org/10.1016/0009-2614\(76\)85294-3](https://doi.org/10.1016/0009-2614(76)85294-3)
36. G.R. Möhlmann, F.J. de Heer, J. Los, Emission cross sections of Balmer- α , β , γ radiation for electrons (0–2000 eV) on H_2 and D_2 . *Chem. Phys.* **25**, 103–116 (1977). [https://doi.org/10.1016/0301-0104\(77\)87067-5](https://doi.org/10.1016/0301-0104(77)87067-5)

Springer Nature or its licensor (e.g. a society or other partner) holds exclusive rights to this article under a publishing agreement with the author(s) or other rightsholder(s); author self-archiving of the accepted manuscript version of this article is solely governed by the terms of such publishing agreement and applicable law.